

Phase-space distribution of relaxed galactic DM component

Mihael Petač

Supervised by Piero Ullio

Astroparticle physics group
SISSA, Trieste

June 23, 2019

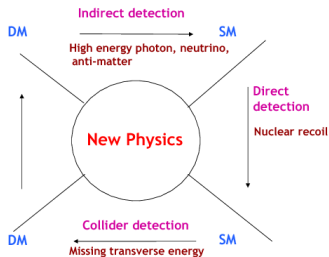
Introduction

Strong evidence for existence of particle-like DM:

- Supported by **independent observations** (e.g. galactic rotation curves, gravitational lensing, CMB)
- Alternative explanations can not account for all the phenomena

Numerous experimental searches for DM particle:

- Collider searches
- Direct detection
- Indirect detection



Current constraints

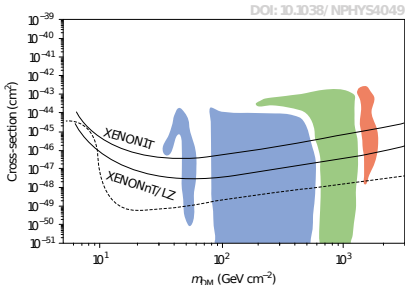
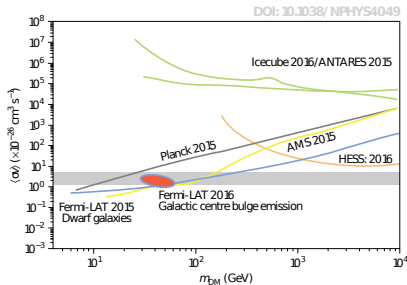


Figure: Indirect detection constraints on annihilation cross-section (left) and direct detection constraints on spin independent DM-nucleon cross-section (right).

Research outline

Motivation:

- Era of **high precision experiments** (Planck, Fermi-LAT, Xenon1T, Gaia ...)
- Direct and indirect detection signals generically depend on **DM velocity distribution**

Outline:

- Obtain self-consistent **DM halo phase-space distribution**
- Address general **velocity dependent cross-sections** (DM-nucleus or DM annihilation)
- Analyze some of the prime targets: **Milky Way** and its **dwarf satellite galaxies**

Indirect detection

Search for high energy particles produced in DM annihilations (or decays) → focus on annihilations into γ -rays

Differential photon flux produced by annihilations:

$$\frac{d\Phi}{dE_\gamma} = \frac{1}{8\pi m_\chi^2} \frac{dN}{dE_\gamma} \int d\Omega \int dl \int d^3v_1 f(\vec{r}, \vec{v}_1) \int d^3v_2 f(\vec{r}, \vec{v}_2) \cdot (\sigma v_{\text{rel}})$$

- **Phase-space distribution** of DM needed for accurate prediction of annihilation flux
- Annihilation cross-section velocity dependence - phenomenologically motivated **Sommerfeld enhancement**:
 $\langle \sigma v_{\text{rel}} \rangle_0 \rightarrow \langle \sigma v_{\text{rel}} \rangle_0 \cdot S(v_{\text{rel}})$

Phase-space distribution functions

For a **spherically symmetric** system there exists an unique **ergodic** (hence isotropic) phase-space distribution function:

$$f(\mathcal{E}) = \frac{1}{\sqrt{8\pi^2}} \frac{d}{d\mathcal{E}} \int_0^{\mathcal{E}} \frac{d\Psi}{\sqrt{\mathcal{E} - \Psi}} \frac{d\rho}{d\Psi} \quad , \quad \mathcal{E} = \Psi(r) - \frac{v^2}{2}$$

Similar expressions can be obtained also for **anisotropic** velocity distributions, where $\beta(r) \equiv 1 - \frac{\sigma_t^2}{2\sigma_r^2} \neq 0$:

- Osipkov-Merritt model: $\beta(r) = \frac{r^2}{r^2 + r_a^2}$
 $f(\mathcal{E}) \rightarrow f(Q = \mathcal{E} - \frac{L^2}{2r_a^2}) \quad , \quad \rho \rightarrow \left(1 + \frac{r^2}{r_a^2}\right) \rho$
- Constant orbital anisotropy: $\beta(r) = \beta_c$
 $f(\mathcal{E}) \rightarrow f_{\beta_c}(\mathcal{E}) \cdot L^{-2\beta_c}$

DM velocity distribution

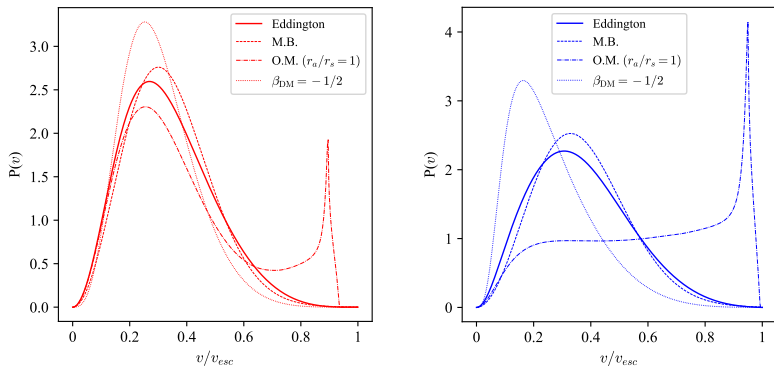


Figure: Velocity distributions computed under different assumptions for NFW (left) and Burkert (right) density profiles.

Application: Milky Way satellites

Dwarf spheroidal galaxies (dSph) present one of the prime targets for detection of DM annihilation events:

- **DM dominated** objects; $10 - 100\times$ higher mass to luminosity ratio than in regular galaxies
- Relative **proximity** of MW dwarfs
- Expecting **small DM velocities**

Strong **Fermi-LAT** constraint on annihilation flux

Stellar distribution and velocity dispersion measurements allow for **reconstruction of gravitational potential** \rightarrow DM density profile

Special thanks to M. Walker for providing us with the pruned data

Application: Bayesian analysis of dSph

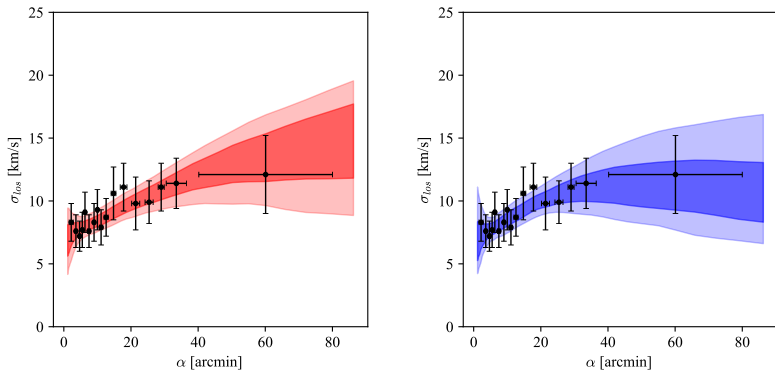
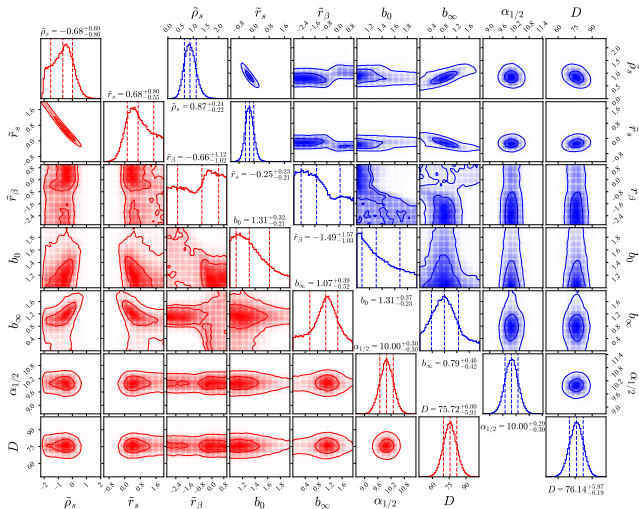


Figure: Draco line-of-sight velocity dispersion data and 68% and 95% credibility intervals for fits using NFW (left) and Burkert (right) profile.

Application: Bayesian analysis of dSph



Application: J-factors

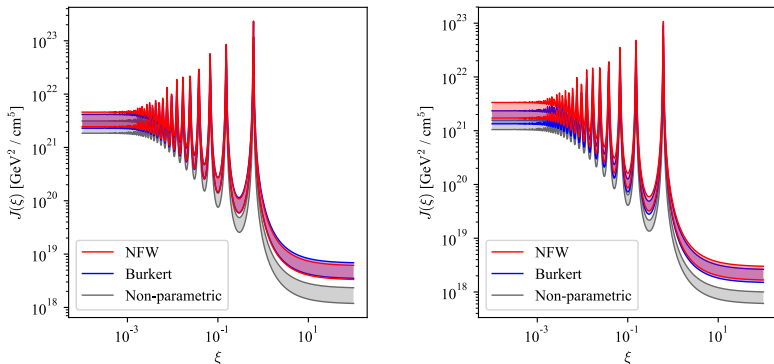


Figure: 68% credibility band for J -factors as a function of $\xi = \frac{m_\phi}{\alpha_\chi m_\chi}$ for Draco (left) and Sculptor (right).

Application: J-factors

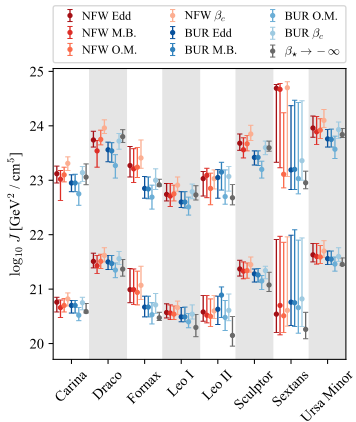
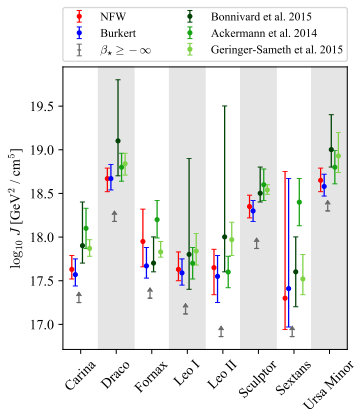


Figure: J -factors for 8 dSph with the 68% confidence intervals.

Summary

Bayesian inference of the dSph **DM halo parameters**.

Careful analysis of **J -factors** in presence of Sommerfeld enhancement with **consistent error propagation**.

Novel results for various DM orbital anisotropies.

Conclusions:

- In presence of Sommerfeld enhancement the dSph constraints on $\langle\sigma v\rangle_0$ strengthen by $\mathcal{O}(10^3)$ - $\mathcal{O}(10^5)$
- Systematic uncertainties due to DM orbital anisotropy at the level of observational uncertainties

Axisymmetric modelling

To address **DM searches in spiral galaxies** one needs to go beyond the spherical approximation

- Direct detection rates in Milky Way
- Indirect detection in the galactic center or nearby spirals

Even if DM halo spherically symmetric, the **gravitational potential is significantly flattened due to baryonic disc!**

Numerous tracers of gravitational potential:

- Gas: rotation curves
- Stars: various disc and halo populations
- Globular clusters & satellite galaxies

Axisymmetric modelling

Stationary solution of Boltzmann equation \Leftrightarrow **relaxed system**

Allows for self-consistent modelling of **additional features**:

- Presence of baryonic disc
- Halo flattening
- Halo rotation

Possible non-relaxed components:

- Debris flow

Necib L. et al.: [arXiv:1810.12301](https://arxiv.org/abs/1810.12301)

- Substructure

Phase-space distribution function

Assume that the phase-space distribution is fully described by **two integrals of motion**

- 1 Relative energy: $\mathcal{E} = \Psi(r) - \frac{v^2}{2}$
- 2 Angular momentum around z-axis: $L_z = R \cdot v_\phi$

$$\Rightarrow f(\mathcal{E}, L_z) = f_+(\mathcal{E}, |L_z|) + f_-(\mathcal{E}, L_z)$$

$$f_+(\mathcal{E}, L_z) = \frac{1}{4\pi^2 i \sqrt{2}} \oint_{C(\mathcal{E})} \frac{d\xi}{\sqrt{\xi - \mathcal{E}}} \frac{d^2 \rho(R^2, \Psi)}{d\Psi^2} \Bigg|_{\substack{\Psi=\xi \\ R^2 = \frac{L_z^2}{2(\xi - \mathcal{E})}}$$

$$f_-(\mathcal{E}, L_z) = \frac{\text{sign}(L_z)}{8\pi^2 i} \oint_{C(\mathcal{E})} \frac{d\xi}{\xi - \mathcal{E}} \frac{d^2 (\rho \bar{v}_\phi)}{d\Psi^2} \Bigg|_{\substack{\Psi=\xi \\ R^2 = \frac{L_z^2}{2(\xi - \mathcal{E})}}$$

Sample spiral galaxy model

- ① **Spherical bulge** (Hernquist potential):

$$\Psi_{\text{bulge}}(R^2, z^2) = \frac{GM_b}{\sqrt{R^2 + z^2 + a_b}}$$

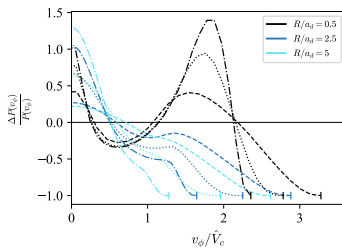
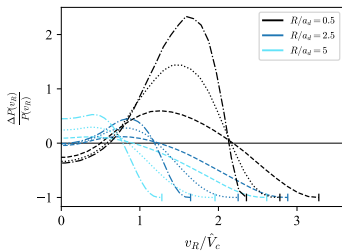
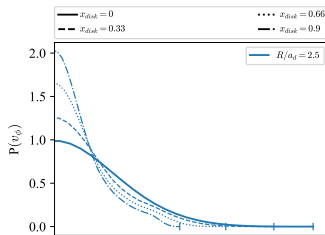
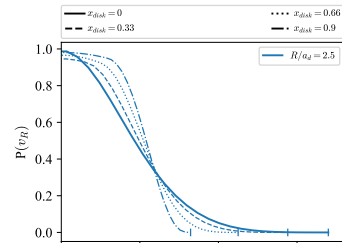
- ② **Axisymmetric disc** (Myamoto-Nagai potential):

$$\Psi_{\text{disc}}(R^2, z^2) = \frac{GM_d}{\sqrt{R^2 + (a_d + \sqrt{z^2 + b_d^2})^2}}$$

- ③ **Axisymmetric halo** (spheroidal NFW profile):

$$\rho_{\text{DM}}(m) = \frac{\rho_s}{m/r_s \cdot (1 + m/r_s)^2} \quad \text{where} \quad m^2 = R^2 + z^2/q^2$$

Disc normalization



Halo rotation

Highly unconstrained

S. E. Bryan et al.: [MNRAS 429, 3316 \(2013\)](#)

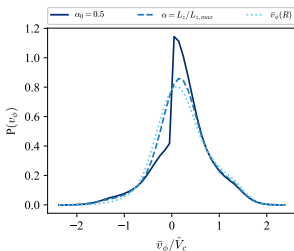
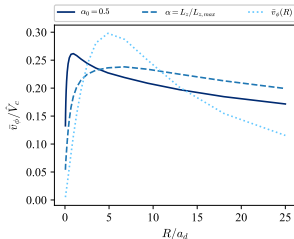
Chua et al.: [MNRAS 484, 476 \(2019\)](#)

Simulations predict spin parameter:

$$\lambda(r) \equiv \frac{J(r)}{\sqrt{2r} M_{\text{DM}}(r) V_c(r)} \sim 0.03 - 0.07$$

Consider several choices:

- 1 $f_-(\mathcal{E}, L_z) = \alpha_c \cdot \text{sign}(L_z) \cdot f_+(\mathcal{E}, L_z)$
- 2 $f_-(\mathcal{E}, L_z) = \frac{L_z}{|L_{z,\text{max}}|} \cdot f_+(\mathcal{E}, L_z)$
- 3 $\bar{v}_\phi(R) = \frac{\omega R}{1 + R^2/r_a^2}$



Direct detection

Attempts to measure **nuclear recoils** in laboratory targets due to interactions with **galactic DM**

$$\frac{dR}{dE_r} = \frac{1}{m_A m_\chi} \cdot \int_{|\vec{v}| > v_{\min}} d^3 v f(\mathcal{E}, L_z) \cdot v \cdot \frac{d\sigma}{dE_r} \quad , \quad v_{\min} = \sqrt{\frac{m_A E_r}{2\mu_{A\chi}^2}}$$

Spin-independent interaction: $\frac{d\sigma}{dE_r} = \frac{m_A \sigma_n^{\text{SI}}}{2\mu_{A\chi}^2 v^2} A^2 F^2(E_r)$

For general $\frac{d\sigma}{dE_r}$ useful to define:

$$g(v_{\min}) \equiv \frac{1}{\rho_\odot} \int_{|\vec{v}| > v_{\min}} d^3 v \frac{f(\mathcal{E}, L_z)}{v}$$

$$h(v_{\min}) \equiv \frac{1}{\rho_\odot} \int_{|\vec{v}| > v_{\min}} d^3 v v \cdot f(\mathcal{E}, L_z)$$

Application: Milky Way model (Bovy2015)

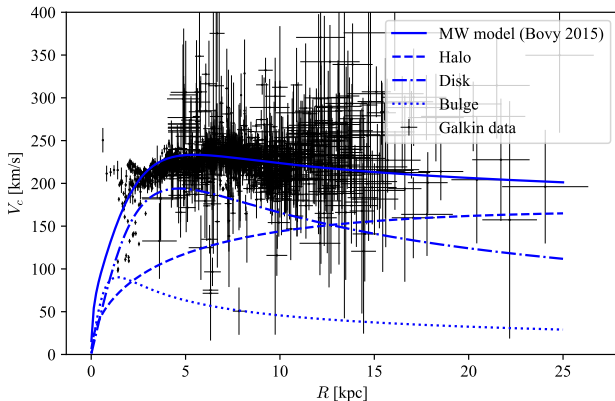


Figure: Comparison of the Milky Way model to the circular velocity data.

Application: Direct detection

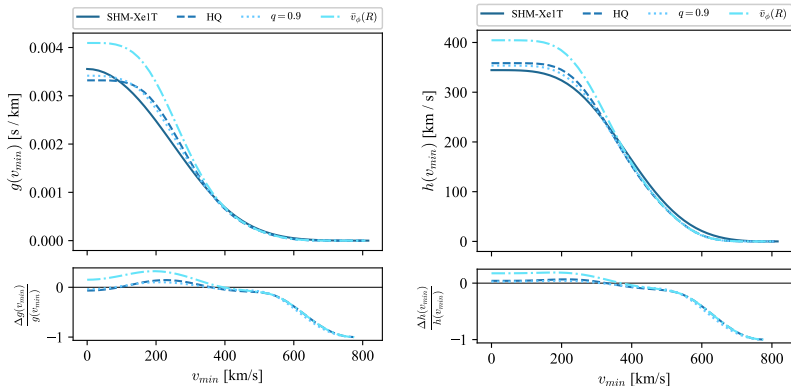


Figure: Dependence of the differential recoil rate on the DM velocity distribution for $\frac{d\sigma}{dE_r} \propto v^{-2}$ (left) and $\frac{d\sigma}{dE_r} \propto v^0$ (right).

Application: Cross-section limits

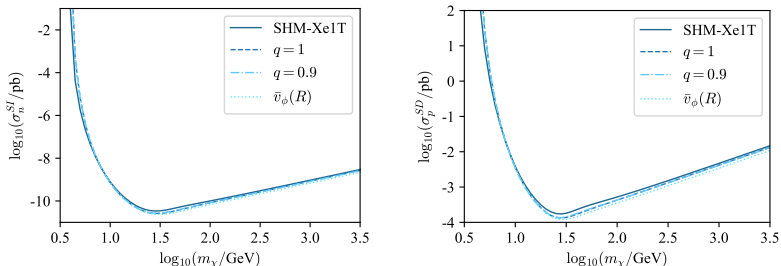


Figure: Cross-section limits for spin-independent (left) and spin-dependent (right) scattering operator.

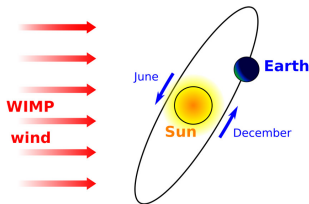
Application: Annual modulation

Annual modulation of $\frac{dR}{dE_r}$ expected due to the **Earth's relative movement** with respect to the galactic rest frame.

Additional boost ($v_{\oplus} \approx 30$ km/s):

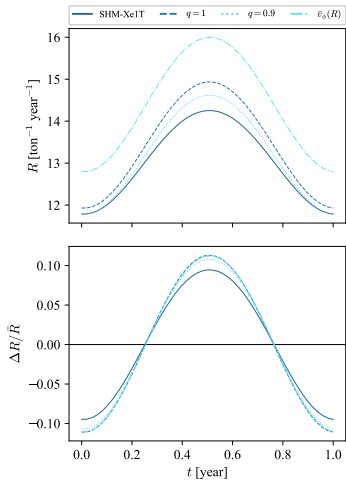
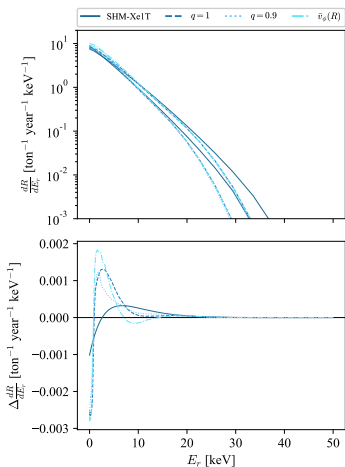
$$\mathcal{E} \rightarrow \mathcal{E} - \frac{v_{\oplus}^2}{2}$$

$$L_z \rightarrow L_z + R_{\odot} (\vec{v}_{\oplus} \cdot \hat{e}_{\phi})$$



Upon detection could provide new information regarding the Milky Way's halo and/or type of DM-nucleon coupling.

Application: Annual modulation



Summary

Implementation of **novel method for phase-space reconstruction in axisymmetric systems.**

Study of **additional halo features:**

- Influence of flattened disc potential
- Halo flattening
- Halo rotation

Reinterpretation of **DM-nucleus cross-section limits.**

Effects of DM phase-space modelling on **annual modulation.**

Conclusion

Rapid **improvements in sensitivity of experiments** call for refined modelling of DM distribution within galaxies.

Detailed analysis needed for:

- **Interpretation of tensions** among different experiments (Galactic center excess, DAMA annual modulation signal)
- **Legitimate exclusion of DM models**

Precise understanding of modelling crucial upon eventual detection of DM signals.

Sommerfeld enhancement

Generic **non-perturbative boost of cross-section** for non-relativistic particles in presence of light force mediator:

$$m_\phi \ll \alpha_\chi m_\chi \quad \text{and} \quad E_\chi \approx m_\chi$$

Coupling of the mediator to DM gives rise to **Yukawa potential**:

$$V(r) = \mp \frac{\alpha_\chi}{r} \exp(-m_\phi r)$$

Solve Schrödinger equation to obtain the **wave function distortion** due to the mediator exchange:

$$\chi''(x) + \left(\frac{v_{\text{rel}}^2}{\alpha_\chi^2} + V(x) \right) \chi(x) = 0 \quad \Rightarrow \quad S(v_{\text{rel}}; \xi) = \left| \frac{\chi(0)}{\chi(\infty)} \right|^2 \propto \frac{1}{v_{\text{rel}}^\alpha}$$

Application: Bayesian analysis of dSph

Observations provide us with **projected surface brightness** Σ_* and **line-of-sight velocity dispersion** $\sigma_{\text{los}}(R)$.

Using Jeans analysis one can compute the σ_{los} for a given model:

$$\sigma_{\text{los}}^2(R) = \frac{1}{\Sigma_*(R)} \int_{R^2}^{\infty} \frac{dr^2}{\sqrt{r^2 - R^2}} \left(1 - \beta_*(r) \frac{R^2}{r^2} \right) p_{r_*}(r)$$

$$p_{r_*}(r) = G_N \int_r^{\infty} dx \frac{\rho_*(x) M_{\text{tot}}(x)}{x^2} \exp \left[2 \int_r^x dy \frac{\beta_*(y)}{y} \right]$$

Use the following likelihood for radially binned data:

$$\mathcal{L}_{\text{kin}} \equiv \prod_{k=1}^N \frac{1}{\sqrt{2\pi} \Delta\sigma_{\text{los}}(k) (\alpha(k))} \exp \left[-\frac{1}{2} \left(\frac{\bar{\sigma}_{\text{los}}(k) - \sigma_{\text{los}}(\alpha(k))}{\Delta\sigma_{\text{los}}(k) (\alpha(k))} \right)^2 \right]$$